ARTICLE NO. 79-1498R

J80-148

Investigation of Three-Dimensional Shock/Boundary-Layer Interactions at Swept Compression Corners

20003
20015
20017

Gary S. Settles,* Jeffrey J. Perkins,† and Seymour M. Bogdonoff‡
Princeton University, Princeton, N.J.

This paper presents the first phase of an experimental study of a three-dimensional shock wave/turbulent boundary-layer interaction at a swept compression corner. Compression corners of 16 and 24 deg angles, which cause near-incipient and well-separated two-dimensional flows at Mach 3, are systematically swept through angles up to 50 deg while maintaining a constant streamwise corner angle. The resulting three-dimensional flows are studied by way of detailed surface measurements and a few exploratory flowfield surveys. Tests of four Reynolds numbers reveal that a Reynolds number influence on the interaction length remains in effect across the available range of sweep. Cylindrical symmetry is obtained along the compression corner at many of the conditions tested. The corner flow differs little from the two-dimensional case for sweep angles less than about 10 deg, above which the interaction length begins to increase dramatically. This increase agrees qualitatively with the assumption of two-dimensional flow normal to the swept corner. Flowfield surveys show that the boundary layer breaks away from the surface to form a free layer at sweep angles up to at least 40 deg. Further, measured yaw angles within the swept interaction deviate only a few degrees from the streamwise direction except near the model surface.

Nomenclature

c_f = skin friction coefficient
ℓ, L = length
L_{incep} = length along corner from upstream boundary required for the inception of cylindrical flow
M = Mach number
Re = Reynolds number
u = velocity
x = distance along test surface in freestream direction, measured from plate leading edge or corner location
y = distance normal to test surface in z = constant planes
z = transverse distance normal to x-axis measured from left edge of corner model
α = compression corner angle in streamwise direction
δ = boundary layer thickness
δ_{avg} = average incoming boundary layer thickness, used to account for spanwise δ variation ahead of swept compression corners
λ = sweep angle of compression corner
ξ = $z/\cos\lambda$, coordinate parallel to compression corner
σ = angle of displacement surface of secondary flow ahead of corner, measured in z = constant planes
ϕ = angle of limiting streamlines on compression ramp
Ψ = angle of limiting streamlines in secondary flow region

Subscripts

c = corner
m, max = location of maximum upstream influence from corner
n = normal to compression corner
r = reattachment
s = separation
0 = initial, incoming boundary-layer condition
∞ = freestream

Presented as Paper 79-1498 at the AIAA 12th Fluid and Plasma Dynamics Conference, Williamsburg, Va., July 23-25, 1979; submitted Aug. 2, 1979; revision received Dec. 17, 1979.

Index categories: Supersonic and Hypersonic Flow; Boundary Layers and Convective Heat Transfer—Turbulent; Shock Waves and Detonations.

*Professional Research Staff Member and Lecturer, Gas Dynamics Laboratory, Dept. of Mechanical and Aerospace Engineering. Member AIAA.

†Graduate Research Assistant, Gas Dynamics Laboratory, Dept. of Mechanical and Aerospace Engineering.

‡Professor and Chairman, Dept. of Mechanical and Aerospace Engineering. Fellow AIAA.

Introduction

THE classical problem of a shock wave interacting with a turbulent boundary layer continues to defy any comprehensive analysis. Progess has been made, however, in the experimental definition and the numerical computation of nominally two-dimensional (2D) shock wave/boundary layer flows. The behavior of such flows is now at least partially understood. In contrast, three-dimensional (3D) shock/boundary layer interactions have received relatively little attention and are barely understood at all. The motivation to gain some understanding in this area can be found in the preponderance of practical aerodynamic applications which are often compressible and almost always turbulent and three-dimensional.

Among the 3D studies which have been carried out, several are concerned with a shock wave swept across a planar boundary layer. The recent publications of Oskam[1] and Peake[2] contain summaries of past work on this problem. Oskam's experimental study demonstrated that conventional 2D scaling laws are inappropriate for a highly swept interaction. This was confirmed by Dolling,[3] who found that the interaction size is independent of the incoming boundary layer thickness for both curved and planar swept shocks. The features of such swept shock flows were recently predicted with some success by Horstman[4] in a numerical solution of the time-averaged Navier-Stokes equations with a turbulence model.

Other 3D shock/boundary-layer studies include Stalker,[5] who found cylindrical symmetry in a swept step experiment. Avduyevskiy and Gretsov[6] obtained overall measurements of the interaction due to a half-cone mounted on a flat plate. Bachalo[7] studied the (mainly laminar) flow about a swept compression corner, including both surface and flowfield measurements.

The swept compression corner geometry has some advantages for a 3D experimental study. It has direct application in the aerodynamics of farings, inlets, and deflected control surfaces on swept wings. The limiting case of the 2D compression corner is reasonably understood,[8] although some underlying physics and the details of the turbulent fluctuations are still missing. The latest methods of numerical computation[9,10] are able to predict attached 2D corner flows, but not the separated case. The 3D compression corner is yet to be studied experimentally with a well-defined compressible turbulent boundary layer. Except for the laminar case,[11,12] corresponding analytical or numerical studies have not been carried out.

The present experimental study was designed as a first step toward filling this gap in the documentation and understanding of 3D compressible flows. An exploratory test program was carried out to measure the effect of progressively sweeping an initially 2D separated compression corner flow. All other parameters were initially held constant during this process, including the streamwise corner angle. Particular emphasis was then placed on examining the effects of variable Reynolds number and variable streamwise corner angle. The applicability of 2D scaling laws to the swept flow in planes normal to the corner was considered. The conditions required for cylindrical symmetry of the interaction were studied. Finally, some exploratory measurements of the flowfield structure were made.

Experimental Procedures

Wind Tunnel and Models

These experiments were done in the Princeton University 20×20 cm High Reynolds Number Supersonic Tunnel. This facility uses high pressure air storage in an intermittent blowdown mode of operation. Length Reynolds numbers up to 1 billion, spanning the range of full-scale flight, can be obtained at Mach 3 under adiabatic wall conditions.

The turbulent boundary layer for this study was developed on a flat plate mounted in the first section of the 20×20 cm tunnel, just aft of the nozzle exit (see Fig. 1). Tests were made at two stations along this plate. Stations 1 and 2 correspond to the transverse datum lines at $x = 17.0$ and 29.7 cm, respectively, from the plate leading edge. Regardless of sweep angle, the edges of all compression corner models mounted on the plate were coincident at one or the other of two points defined by the intersections of the transverse datum lines with a streamwise datum line at 7.62 cm from the left sidewall of the wind tunnel.

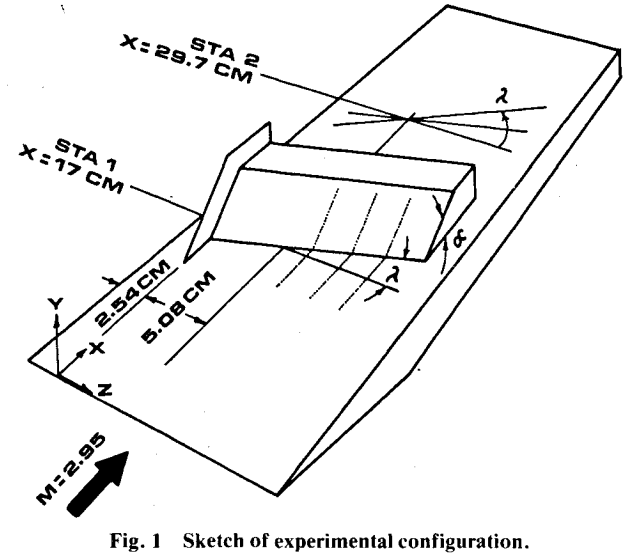

Fig. 1 Sketch of experimental configuration.

Individual compression corner models were progressively swept in a counter-clockwise direction, as shown in Fig. 1, so that the left side of the model was always "upstream." All models were cut away 2.54 cm from the wind tunnel sidewalls to avoid the sidewall boundary layers. Aerodynamic fences were placed at these edges, as described later.

Both the plate and the ramp models were instrumented with streamwise rows of surface pressure taps. These taps were 0.54 mm in diameter, and were spaced a minimum of 0.64 mm apart. The streamwise tap rows were located at $z = 6.99$, 9.53, and 12.07 cm for the $\alpha = 16$ deg corner models, and at $z = 5.08$, 8.89, and 12.70 cm for the $\alpha = 24$ deg models.

Two streamwise compression corner angles were considered: $\alpha = 16$ and 24 deg. For each α, models were built with sweep angles $\lambda = 0$, 5, 10, 20, 30, and 40 deg. Since it was desired to maintain a constant streamwise compression corner angle regardless of sweep, a different test model was required for each sweep angle.

Some additional tests were made with a model defined by $\alpha = 24$ deg and $\lambda = 50$ deg, but surface pressure measurements for $\alpha = 24$ deg were limited to sweep angles $\lambda = 0$, 5, and 10 deg. Selected models were also built such that they were swept back through the same λ angle on both sides of an apex located at the $z = 5.08$ cm datum line.

Test Conditions and Boundary Layer

The tests were carried out at a freestream Mach number of 2.95 and a stagnation temperature of 268 K $\pm$ 4%. The model wall condition was approximately adiabatic. Four test Reynolds numbers were obtained through the combination of two x stations and two values of Re_∞. Natural transition occurred within about 2 cm of the plate leading edge at these moderately high Reynolds numbers. The Reynolds number conditions and the corresponding values of δ_0 are summarized in Table 1.

An average incoming boundary layer thickness, δ_{avg}, was used in some circumstances to account for the streamwise growth of δ before encountering a swept corner line. This average spanwise δ was evaluated at the intersection of the central pressure tap row and the position of the particular corner under consideration.

The mean velocity profile of the turbulent boundary layer at $x = 24.6$ cm and $Re_\infty = 6.3 \times 10^7$/m is shown in Fig. 2. The profile is matched by the standard wall-wake similarity law.[14] This is taken as evidence that the boundary layer is an equilibrium condition and is thus free of upstream history effects.

Instrumentation and Techniques

The present mean flow measurements included surface pressures which were collected by a Scanivalve, digitized, and plotted on-line using an HP1000 minicomputer. A streamlined pitot probe with a tip height of 0.25 mm was used for the boundary layer surveys. Some preliminary flowfield measurements were made with a miniature 3-hole "cobra" yaw probe, using techniques which are fully described by

Table 1 Reynolds number and boundary layer test conditions

Re_∞/m	x, cm	Re_x	δ_0, cm	$Re_{\delta 0}$
6.30×10^7	17.0	1.07×10^7	0.22	1.4×10^5
6.30×10^7	29.7	1.87×10^7	0.35	2.2×10^5
1.87×10^8	17.0	3.18×10^7	0.21	3.9×10^5
1.87×10^8	29.7	5.55×10^7	0.33	6.2×10^5

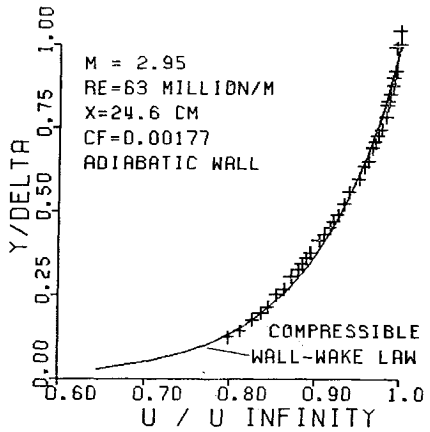

Fig. 2 Incoming turbulent boundary layer mean-velocity profile compared with Coles' wall-wake law.

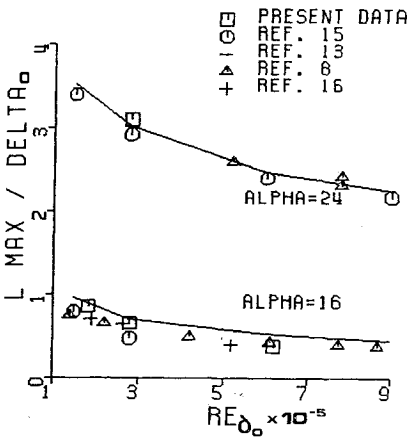

Fig. 3 Upstream influence of 2D compression corners and Reynolds number effect at Mach 3.

Oskam.[1] The probe tip was 0.41 mm high by 2 mm wide, and was continuously nulled into the local flow direction.

Surface flow patterns were obtained by a kerosine-graphite streak method (Ref. 8, Appendix B). Briefly, this mixture coats the test surface during a run and then evaporates. Only a microscopic layer of graphite remains to display the surface streak angles. This layer is lifted off using large squares of transparent adhesive tape, and is preserved by pressing it on white paper. The resulting trace is full-sized, undistorted, and very detailed. This technique avoids the buoyancy problems that may affect standard fluorescent oil patterns. Streak distances and angles can be measured directly from kerosine-graphite traces, yielding quantitative information. Even so, such surface traces by themselves supply only a fraction of the information needed to define a flowfield.

Results and Discussion

End Effects

Careful consideration of end effects is even more important here than in nominal 2D flows, since 3D cross-flows may carry an influence of the left and right edges of the corner model throughout the field of measurement. The present strategy to avoid such problems involves the use of a large experimental aspect ratio (a corner span of up to 70 boundary layer thicknesses). In addition, the following checks were made.

The test program began with "apex" corner models which were swept back on both sides of an x-y plane of symmetry, as in Ref. 7. The symmetry plane was then replaced by a small aerodynamic fence shown in Fig. 1. For a number of test cases the apex models and full-span fenced models gave nearly identical surface flow patterns and pressure distributions. Thereafter the apex models were abandoned in order to gain a greater aspect ratio with the full-span corner geometry.

A similar strategy was applied at the right-hand, or "downstream" boundary of the swept corners. A streamwise fence was required here at low sweep angles to avoid spillage of the separated flow. At higher sweep angles the downstream fence could be omitted, its spanwise influence being only a few boundary layer thicknesses at most.

Limiting Case of 2D Flow

Quite a few experimental and theoretical studies of the 2D compression corner interaction have been performed. The state of the art is summarized in at least two recent reports.[8,13] The gross effects of changes in M, Re, and α are known. The 16 and 24 deg compression corner angles of the present study are known to cause near-incipient and well-separated 2D flows, respectively, at Mach 3. Some verification of the present results can be had by comparing with these established trends for the limiting case of $\lambda = 0$ deg.

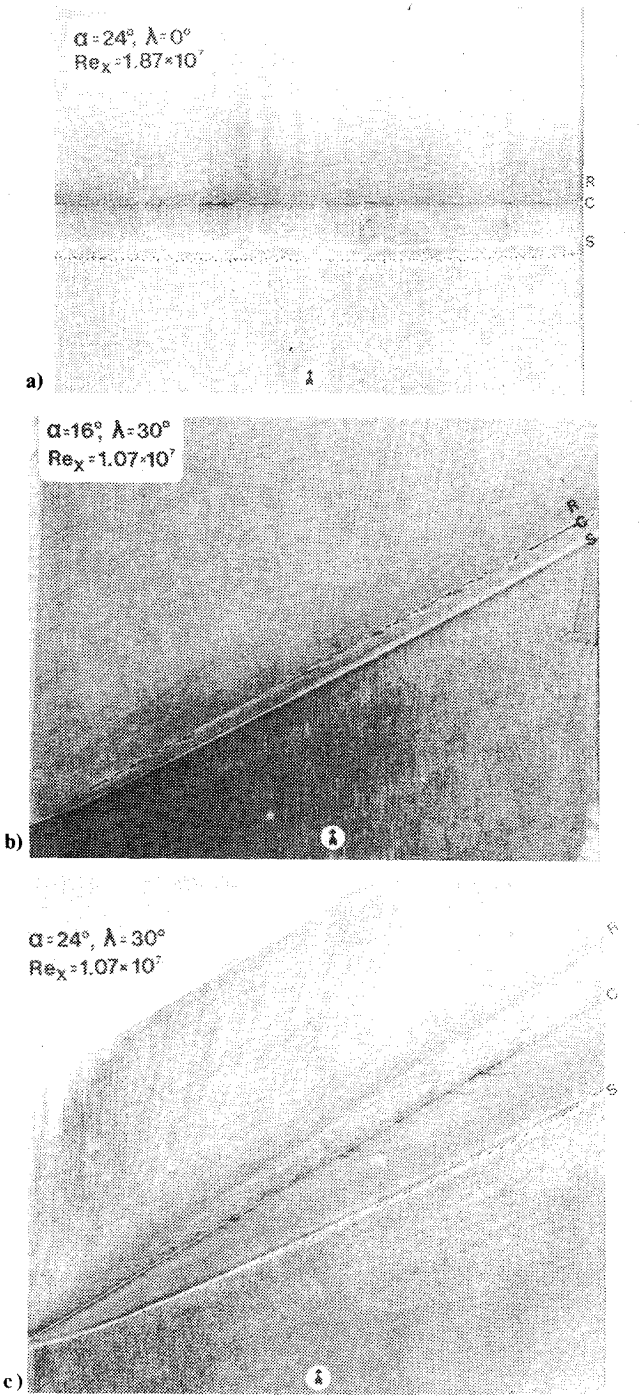

Fig. 4 Examples of kerosine-graphite surface flow patterns on 2D and swept compression corners.

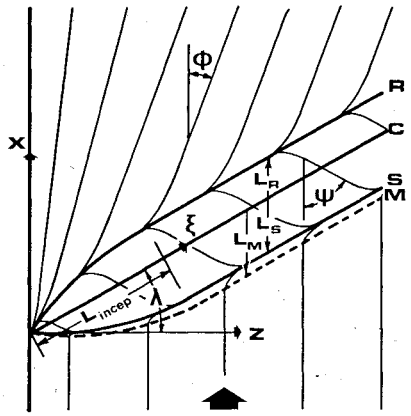

Fig. 5 General sketch of surface flow pattern on swept compression corner with definition of parameters.

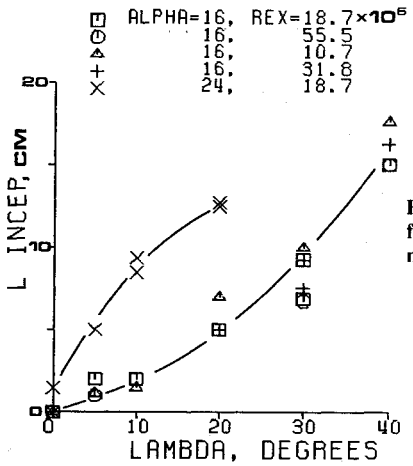

Fig. 6 Inception length for cylindrically symmetric corner flow.

Such a comparison is shown in Fig. 3, where the compression corner upstream influence data from five separate studies (Refs. 8, 13, 15, and 16 and the present data) are plotted vs Re_{δ_0}. This constitutes remarkable agreement among experiments in disparate wind tunnels ranging in test section scale from 0.05-1.2 m.

The solid line in Fig. 3 is a correlation of experimental data obtained by Roshko and Thomke[13] over ranges of α, M, and Re. The latter two parameters are accounted for by the skin friction coefficient in the correlation equation,

$$\ell_m/\delta_0 = 10^3\,(\alpha/18.29)^{2.81}\,[c_{f_0} - 10^{-3}\,(1.0 - 0.001189\alpha^2)] \quad (1)$$

Figure 3 verifies that the present results for zero sweep are consistent with established 2D trends. It also clearly shows that δ_0 is a proper scaling parameter for 2D compression corner interaction lengths.

Surface Flow Patterns

Examples of kerosine-graphite surface flow patterns are shown in Fig. 4. The streak lines are believed to represent limiting streamlines of the flowfield.[17]

Assuming that the limiting streamline interpretation does apply, the surface flow pattern results indicate that the 2D lines of separation and reattachment in the zero-sweep case become 3D lines of separation and reattachment once sweep is introduced. This would be a questionable interpretation if based only on surface patterns. Further data and discussion supporting this interpretation are given in sections to follow.

Early in the investigation the authors speculated that the addition of sweep might cause the secondary flow at the initially 2D compression corner to bleed away in the spanwise direction and to disappear. The surface flow pattern data clearly demonstrate that this is not the case. Instead, the scale

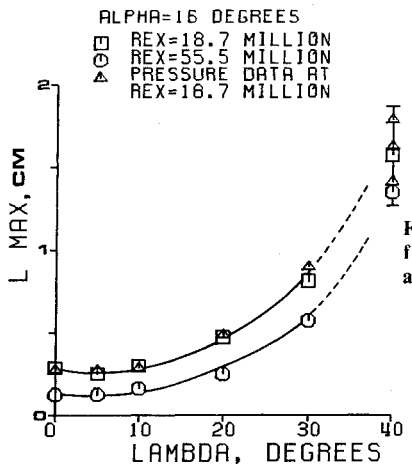

Fig. 7 Upstream influence length vs sweep angle for 16 deg corner.

of the indicated secondary flow increases with higher sweep angles.

Strong cross-flows of the limiting streamlines develop near the lines of streak convergence and divergence (henceforth referred to as lines of separation and reattachment). The resulting overall pattern of limiting streamlines is similar to the pattern observed by Bachalo[7] and corresponds to Maskell's[18] definition of "bubble-type" 3D separation.

To aid in the discussion of surface flow pattern features, the definitions of several parameters based on the patterns are given on a general diagram in Fig. 5. The quantitative nature of the kerosine-graphite traces allowed the measurements of these parameters with some accuracy and consistency.

Approach to Cylindrical Symmetry

Cylindrically symmetric flow, with the boundaries of the secondary flow region becoming parallel to the compression corner, was found for a number of the present test conditions. Figure 6 shows the inception length for cylindrical flow as a function of corner sweep angle. From these results, the $\alpha = 16$ deg corner flow develops a cylindrical region over the range of sweep angles 0 deg $\leq \lambda < 40$ deg. The $\alpha = 24$ deg corner flow develops a cylindrical region for 0 deg $\leq \lambda < 20$ deg. For greater sweep angles than these, cylindrical symmetry was questionable within the limits of the present experimental geometry.

Such cylindrical symmetry was not often obtained in past 3D interaction studies. While Stalker[5] found cylindrical flow in a swept step experiment, Oskam[1] and the other swept shock investigators did not find it. This may have been due to the lack of a sufficiently long test geometry in the sweep direction. Alternatively, it might reflect a tendency toward conical symmetry ($L_{incep} \to \infty$) at high sweep angles. No such tendency is apparent in Fig. 6 for sweep angles up to at least 40 deg, however.

The inception lengths for cylindrical flow in Fig. 6 are deliberately presented in dimensional form rather than in normalized form. The reason is that the "obvious" normalizer, incoming boundary layer thickness, artificially spreads the data points across the plot because it varies with Reynolds number while the physical inception lengths are essentially independent of Reynolds number. A similar situation has been observed by Dolling,[3] wherein the 3D interaction lengths ahead of a blunt fin in a turbulent bounday layer are scaled by fin diameter but not by incoming δ. These results raise serious questions about the appropriateness of boundary layer thickness as a scaling parameter in some or all 3D flows.

Upstream Influence

The fact that the upstream influence length of the compression corner flow rises as the corner is swept was mentioned in reference to the surface flow pattern data. It is seen

more clearly in Fig. 7, where L_m is plotted vs λ for the 16 deg corner at two Reynolds numbers. These results show little effect of sweep angles up to 10 deg on the upstream influence parameter. Beyond $\lambda = 10$ deg the upstream influence begins to grow rapidly. The effect of a higher Re_∞ in decreasing L_m for the 2D case is preserved for sweep angles up to at least 30 deg.

The trend of the data in Fig. 7 bears a striking similarity to the curve of $\cos\theta$ for 180 deg $\leq\theta\leq$ 220 deg, which suggests the possibility of a direct geometrical relation between upstream influence and sweep angle. This possibility is explored further in the section on quasi-2D flow.

As the compression corner is swept back, the distance from the plate leading edge to a point on the corner model increases. Thus the local incoming boundary layer thickness increases somewhat. However, because δ grows slowly with x and the corner model is rotated about a point near the plate center, the average incoming δ varies only about $\pm 5\%$ for sweep angles up to 40 deg. This variation is far too small to account for the observed upstream influence growth as the corner is swept. Also, normalizing L_{max} by δ_{avg} does not remove the Reynolds number effect shown in Fig. 7. Similar conclusions apply to the $\alpha = 24$ deg data.

Surface Pressure Distributions

The surface pressure distributions which were measured in cylindrical flow regions for $\alpha = 16$ deg and 0 deg $\leq\lambda\leq$ 30 deg, and in noncylindrical flow for $\lambda = 40$ deg, are shown in Fig. 8. Through 30 deg of sweep, the three spanwise tap rows which were read for each sweep angle coincide on the single curves shown, confirming that the flow is cylindrical. Further, the pressure distribution does not change at all from the 2D case for sweep angles up to 10 deg, despite the strong deviation of the limiting streamlines noted in the surface flow patterns. For sweep angles above 10 deg, the interaction grows in the upstream and downstream directions.

The theoretical inviscid pressure rise, toward which all the measured pressures on the ramp face convergence, varies only about 4% for sweep angles up to 40 deg. This theoretical pressure rise is obtained from the classical oblique shock formulas resolved normal to the compression corner. It remains almost fixed because the sweep effects on normal Mach number and normal corner angle are self-compensating. (Clearly, this would not have been the case if the *normal* corner angle, rather than the streamwise angle, had been held constant in this study.)

The effect of sweep angle in Fig. 8 resembles the effect of a large Reynolds number change on a 2D compression corner flow. There, too, the interaction length would change significantly while the final pressure rise remained fixed. However, in that case, the change in interaction length can be related to changing upstream conditions, whereas in Fig. 8 the upstream conditions do not change. This analogy helps to explain why upstream conditions such as δ_0 are not suitable, by themselves, for scaling this 3D interaction.

The surface pressure distributions for cylindrical flow in the $\alpha = 24$ deg corner case are shown in Fig. 9. Here, measurements were made at sweep angles up to 10 deg. As in the 16 deg case, the 24 deg pressure distributions do not change significantly over that range of sweep.

Note that the measured pressures near the corner line ($x = 0$) in Figs. 8 and 9 are invariant with sweep angle. Further, the pressure curves ahead of the corner, being the same as or similar to the 2D case, suggest that the 3D secondary flow at the swept corner exerts a similar displacement on the inviscid stream as in the unswept case. To investigate this similarity further, the angle σ between the plate and a streamwise line connecting the separation and reattachment points has been computed from the following simple trigonometric relation.

$$\sigma = \arctan[\ell_R \sin\alpha / (\ell_R \cos\alpha + \ell_s)] \qquad (2)$$

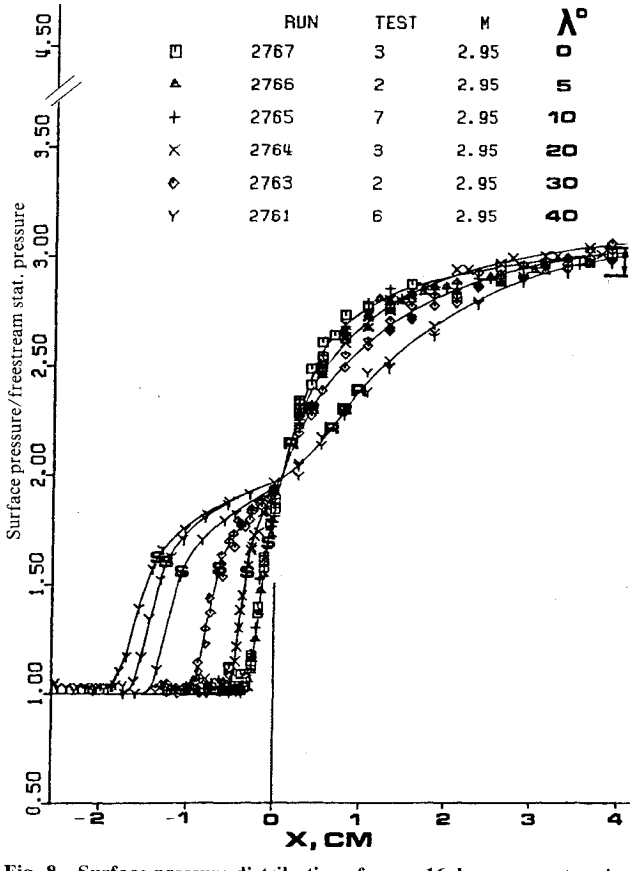

Fig. 8 Surface pressure distributions for $\alpha = 16$ deg corner at various sweep angles, $Re_x = 1.87 \times 10^7$ ($x = 0$ is corner line in each case).

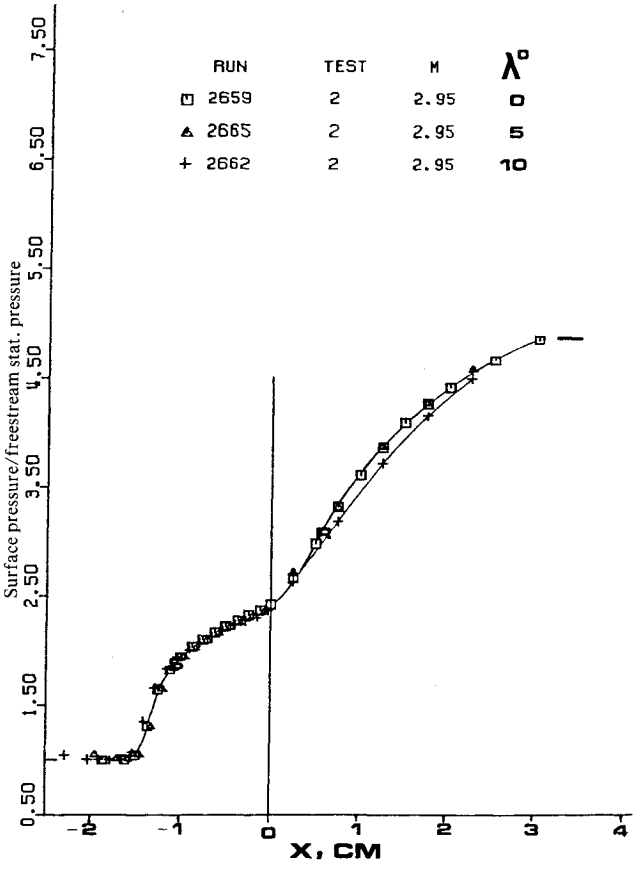

Fig. 9 Surface pressure distributions for $\alpha = 24$ deg corner at various sweep angles, $Re_x = 1.87 \times 10^7$.

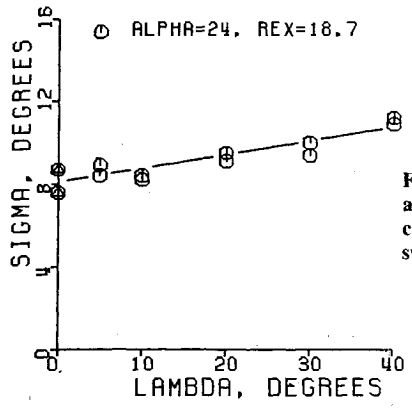

Fig. 10 Displacement angle of compression corner secondary flow vs sweep angle.

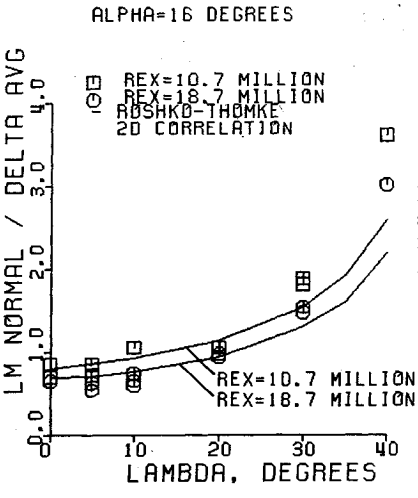

Fig. 11 Comparison of swept corner upstream influence parameter and 2D correlation resolved normal to corner line.

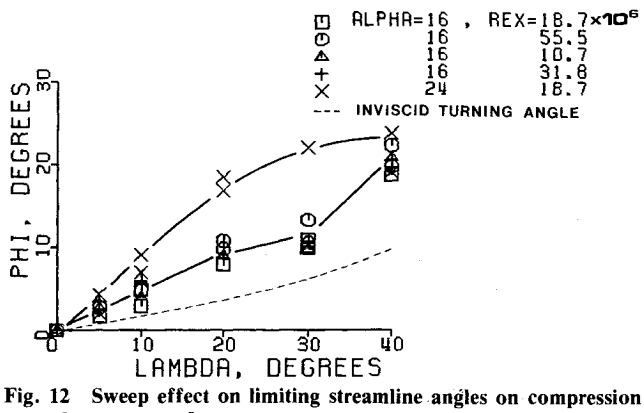

Fig. 12 Sweep effect on limiting streamline angles on compression ramp downstream of corner.

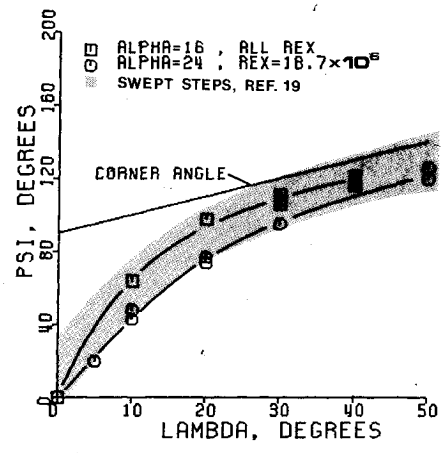

Fig. 13 Sweep effect on limiting streamline angles in secondary flow region.

This "idealized shear layer angle" is plotted vs λ in Fig. 10. It varies only slightly over a sweep range of 0-40 deg. This agrees with the experimental results of Ref. 6, and further supports the notion that the inviscid stream displacement angle ahead of the corner is almost independent of sweep.

Quasi-2D Flow

It has been postulated by some investigators[11] and partially supported by the measurements of others,[5,6] that quasi-2D flow may be assumed in swept shock/boundary layer interactions exhibiting cylindrical symmetry. It is reasoned that, since the interaction is cylindrical, the third dimension along the interaction is degenerate. Thus the problem reduces to one of 2D (planar) flow with a suitable coordinate transformation.

Stalker[5] attempted to correlate his swept step measurements with a simple extension of a 2D analysis resolved normal to the sweep line, and had some success. The same strategy can be tested here, with the reservation that there is no comprehensive analysis available for turbulent interactions, even in the 2D case.

The excellent performance of the Roshko-Thomke correlation (not a theory) in Fig. 3 suggests that it be used for this purpose. Accordingly, Eq. (1) was evaluated at the conditions corresponding to several of the current $\alpha = 16$ deg test points, using the *normal* components of M, Re, and α. The results are compared with the experimental data points in Fig. 11.

As in Fig. 3, the correlation matches the current results at zero sweep angle. As the sweep angle is increased, both the correlation and the measurements show a rise in normalized upstream influence length. The agreement becomes poorer at the higher sweep angles. Nonetheless, the assumption of quasi-2D flow is at least in qualitative agreement with the observed behavior in that it gives the correct trend of upstream influence dependence upon sweep angle. However, much more conclusive evidence would be required to confirm or deny the assumption of quasi-2D flow.

Sweep of Limiting Streamlines

The sweep angles of the limiting streamlines with respect to the x axis were measured from the compression corner surface flow patterns. Figure 12 shows the limiting streamlines angle ϕ on the compression ramp as a function of corner sweep angle λ. The limiting streamline angle grows with increasing λ, reaching values of about 20 deg for 40 deg sweep. It is dependent upon the streamwise compression corner angle but essentially independent of the Reynolds number.

The limiting streamlines are swept on the compression ramp downstream of the position where the final pressure level is reached. This indicates that there is a lingering cross-flow near the bottom of the boundary layer downstream of the swept corner. The limiting streamlines are also swept in regions of cylindrical symmetry where there is no pressure gradient in the ξ direction.

Figure 13 shows the average limiting streamline angle ψ within the secondary flow region as a function of the corner sweep angle. This plot shows that the limiting streamlines deviate immediately from pure flow reversal once a small amount of corner sweep is added to the initially 2D interaction. (Recall that some other gross features of the flowfield, such as the surface pressure distribution and the upstream influence, are unaffected by small sweep angles.) The limiting streamlines of the secondary flow appear to approach asymptotically a condition in which they are inclined only about 10 deg to the corner line at the higher λ angles. Above $\lambda \sim 17$ and 26 deg for $\alpha = 16$ and 24 deg, respectively, the limiting streamlines no longer have "reversed" components with respect to the streamwise direction.

The shaded band in Fig. 13 denotes the ψ angles from unpublished surface flow patterns taken by Stalker[19] during his original 1960 study[5] of swept steps. There is good agreement between the present results and those of Stalker despite the fact that the test geometry, Mach number, and facility were different. This could be taken as a suggestion that these 3D limiting streamlines tend to develop in some universal fashion, which deserves further study.

In an effort to connect the sweep of the limiting streamlines with the yaw angles of the flow about the test surface, several exploratory yaw-probe surveys were made. The general result of these surveys is that the flowfield yaw angles in x-y planes are small throughout the interaction except in the immediate vicinity of the surface. This conclusion agrees with the measurements of Kussoy, Viegas, and Horstman[20] in a similar 3D interaction. Further, the measured yaw-probe angles near the surface on the compression ramp were in good agreement with the limiting streamline angles shown in Fig. 12. Finally, the probe measurements and subsequent tuft studies indicated that a detached shear layer forms above the swept compression corner and connects the measured separation and reattachment lines.

Summary and Conclusions

The first phase of an experimental study of the shock wave/turbulent boundary layer interaction at a swept compression corner is reported in this paper. The study was carried out in adiabatic flow at Mach 3, and over a length-Reynolds number range of 11-55 million. Compression corners of 16 and 24 deg streamwise angles were systematically swept through angles up to 50 deg. The mean flow measurements included surface pressures and streak patterns, and some preliminary flowfield surveys. This exploratory study was designed to gain an overall view of the swept compression corner interaction, and to test the applicability of 2D scaling laws to this 3D interaction phenomenon. Several conclusions and observations have been found, as listed below.

1) The experimental results agree with other nominally 2D experiments for the limiting case of zero sweep angle.

2) Cylindrical symmetry of the corner flowfield was found over a range of the measured test conditions.

3) For sweep angles less than about 10 deg, the characteristics of the interaction do not differ from the zero-sweep case in any respect except that of the limiting streamlines near the surface.

4) The limiting streamlines divert immediately from their 2D configuration once a small amount of sweep is introduced, and remain significantly skewed from the streamwise direction even after the final pressure level of the interaction has been reached.

5) Above 10 deg sweep the interaction lengths increase significantly although the final pressure level remains constant. This increase is not accounted for by the spanwise growth of local incoming boundary layer thickness.

6) There is evidence that the incoming boundary layer thickness is not suitable as a scaling parameter for a swept compression corner flow.

7) The trend of decreasing interaction length with increasing Reynolds number applies to the compression corner flow over a sweep range from 0 to at least 30 deg.

8) Sweep does not significantly change the displacement angle of the outer, inviscid stream above the secondary flow region at the compression corner. As a result of this, the surface pressure in the immediate vicinity of the compression corner remains approximately constant.

9) The assumption of quasi-2D flow normal to interactions with cylindrical symmetry applies, at least qualitatively, to the present results.

10) Exploratory flowfield surveys show that the yaw angles of the swept interaction are small everywhere except in the immediate vicinity of the surface.

11) Surface flow patterns, if taken by themselves, could give the misleading impression that the entire flowfield is highly skewed from the streamwise direction, which is not found to be the case.

Acknowledgment

This work was supported by the U.S. Air Force Office of Scientific Research, Contract F44620-75-C-0080, monitored by Dr. J. D. Wilson.

References

[1] Oskam, B., "Three-Dimensional Flowfields Generated by the Interaction of a Swept Shock Wave with a Turbulent Boundary Layer," Ph.D. Thesis, Dept. of Mechanical and Aerospace Engineering, Princeton Univ., 1976.

[2] Peake, D. J., "The Three-Dimensional Interaction of a Swept Shock-Wave with a Turbulent Boundary Layer and the Effects of Air Injection on Separation," Ph.D. Thesis, Carleton Univ., Ottawa, 1975.

[3] Dolling, D. S, Cosad, C. D., and Bogdonoff, S. M., "An Examination of Blunt-Fin Induced Shock Wave Turbulent Boundary Layer Interactions," AIAA Paper 79-0068, New Orleans, La., Jan. 1979.

[4] Horstman, C. C. and Hung, C. M., "Computation of Three-Dimensional Turbulent Separated Flows at Supersonic Speeds," *AIAA Journal*, Vol. 17, Nov. 1979, pp. 1155-1156.

[5] Stalker, R. J., "Sweepback Effects in Turbulent Boundary-Layer Shock-Wave Interaction," *Journal of the Aeronautical Sciences*, Vol. 27, May 1960, pp. 348-356.

[6] Avduyevskiy, V. S. and Gretsov, V. K., "Investigation of a Three-Dimensional Separated Flow Around Semicones Placed on a Plane Plate," NASA Technical Translation F-13, 578, 1971.

[7] Bachalo, W. D., "Three-Dimensional Boundary Layer Separation in Supersonic Flow," Univ. of California, Berkeley, Rept. FM-74-10, Aug. 1974.

[8] Settles, G. S., "An Experimental Study of Compressible Turbulent Boundary Layer Separation at High Reynolds Number," Ph.D. Thesis, Dept. of Mechanical and Aerospace Engineering, Princeton Univ., Princeton, N.J., 1975.

[9] Horstman, C. C., Settles, G. S., Vas, I. E., Bogdonoff, S. M., and Hung, C. M., "Reynolds Number Effects on Shock-Wave Turbulent Boundary Layer Interactions," *AIAA Journal*, Vol. 15, Aug. 1977, pp. 1152-1158.

[10] Settles, G. S., Fitzpatrick, T. J., and Bogdonoff, S. M., "A Detailed Study of Attached and Separated Compression Corner Flowfields in High Reynolds Number Supersonic Flow," *AIAA Journal*, Vol. 17, June 1979, pp. 579-585.

[11] Vatsa, V. N. and Werle, M. J., "Quasi-Three-Dimensional Laminar Boundary-Layer Separations in Supersonic Flow," *Numerical/Laboratory Computer Methods in Fluid Mechanics*, ASME, 1976, pp. 93-109.

[12] Holt, M. and Modarress, D., "Application of the Method of Integral Relations to Laminar Boundary Layers in Three Dimensions," *Proceedings of the Royal Society*, London, A.353, 1977, pp. 319-347.

[13] Roshko, A. and Thomke, G. J., "Flare Induced Interaction Lengths in Supersonic, Turbulent Boundary Layers," *AIAA Journal*, Vol. 14, July 1976, pp. 873-879.

[14] Matthews, D. C., Childs, M. E. and Paynter, G. C., "Use of Coles' Universal Wake Function for Compressible Turbulent Boundary Layer," *Journal of Aircraft*, Vol. 7, March-April 1970, pp. 137-140.

[15] Law, C. H., "Two-Dimensional Compression Corner and Planar Shock Wave Interactions with a Supersonic, Turbulent Boundary Layer," ARL TR 75-0157, June 1975.

[16] Moy, C. K., "An Experimental Study of Incipient Boundary Layer Separation in Compressible Flow at Low Turbulent Reynolds Numbers," Sr. Thesis, Dept. of Mechanical and Aerospace Engineering, Princeton Univ., Princeton, N.J., May 1978.

[17] Peake, D. J., "Phenomenological Aspects of Quasi-Stationary Controlled and Uncontrolled Three-Dimensional Flow Separations," Paper 5, AGARD-LS-94, Feb. 1978.

[18] Maskell, E. C., "Flow Separation in Three Dimensions," RAE Aero Rept. 2565, Nov. 1955.

[19] Private communication, Prof. R. J. Stalker, Dept. of Mechanical Engineering, University of Queensland, Australia, Sept. 1979.

[20] Kussoy, M. I., Viegas, J. R., and Horstman, C. C., "An Experimental and Numerical Investigation of a 3D Shock Separated Turbulent Boundary Layer," AIAA Paper 80-0002, Pasadena, Calif., Jan. 1980.